Evaluating the "darkness" of melanin materials.

Koen P. Vercruysse

Chemistry Department, Tennessee State University, Nashville, USA

Corresponding author: kvercruysse@tnstate.edu

Abstract: We developed a mathematical process to quantify the apparent darkness of solutions containing melanin-like materials. The visible portion of their UV-Vis spectra is model using an exponential equation. Linear regression analysis provides the constants that define this exponential equation. Using these constants, the exponential equation is integrated between 400nm to 900nm to obtain the area-under-the-curve (AUC) of the visible portion of the UV-Vis spectra. This process was applied to data collected from various melanin-like materials discussed in earlier reports. By comparing the AUC values of different samples one can readily compare the "darkness" of melanins and evaluate the impact varying reaction conditions may have on this physical property. We revisited the results of earlier reports and discuss additional points related to the UV-protective properties attributed to melanins.

Keywords: melanin, catechols, amino acids, L-cysteine, UV protection

1. Introduction

It is well established that the melanogenesis process, the synthesis of melanin-like materials from suitable precursors, is a complex sequence of chemical reactions and physical interactions involving a multitude of intermediates.[1-3] The result of these processes is most often a darkly-colored and enigmatic final product. The enigmatic nature of the melanin pigments (MNs) comes from the fact that, despite decades of research, there is no definitive description of their chemical structure, or a definitive explanation for their dark color. The dark appearance of MNs is exhibited by a monotonic, absorbance profile over the entire ultraviolet (UV) and visible (Vis) range of the electromagnetic spectrum.

This broad-band absorbance feature can be modeled using a logarithmic function as discussed in other reports.[4-6] This mathematical model is shown in the equation below:

$$A = A_0 * e^{-k\lambda} \qquad \textbf{eq.1}$$

In this equation, λ is the wavelength in nm, A is the absorbance at a particular λ, A_0 is the absorbance extrapolated for λ = 0nm and k is a decay constant. **Eq.1** can be transformed into a linear format as is shown in **eq. 2** and the two constants, k and A_0, can readily be obtained through linear regression analysis.

$$\boldsymbol{ln\ A = ln\ A_0 - k\lambda} \qquad \textbf{eq.2}$$

Observations made in our laboratory involving catecholamines, indicated that the melanogenesis process leads to a mixture consisting of components with distinct absorbance peaks within the UV range of the electromagnetic spectrum and a separate set of components that are responsible for the dark appearance of the reaction mixtures.[7] Through a co-precipitation process these two sets of components could be separated and it appeared that the components with absorbance in the UV range do not contribute to the dark appearance of the crude reaction mixtures. Based upon these observations we revisited the UV-Vis spectra of materials reported upon elsewhere. We applied **eq.2** to the visible portion of the UV-Vis spectra of the crude reaction mixtures or the solutions of purified MN-materials. Linear regression analyses according to **eq.2** were performed for the absorbance readings between 500nm and 800nm to avoid the interference of components with strong absorbance in the upper UV regions and to ensure that all absorbance readings involved were sufficiently above baseline. Using the values of k and A_0 derived through linear regression analysis according to **eq.2**, we calculated the area-under-the-curve (AUC) of the sample's absorbance of the entire visible region of the electromagnetic spectrum (400 to 900nm). This AUC can be calculated through an integration of **eq.1** between 400 and 900nm as shown in **eq.3**.

$$\boldsymbol{AUC = \int_{400}^{900} A_0 * e^{-k\lambda} d\lambda = \frac{A_0}{-k} * \left(e^{-k*900} - e^{-k*400}\right)} \qquad \textbf{eq.3}$$

The AUC thus calculated can be used as an objective measure of the "darkness" of any MN sample, e.g., to compare the effect of reaction conditions on the overall appearance of the MN-like materials. In addition, using the values of k and A_0 one can calculate an estimate of the absorbance for any given λ. Subtracting these modeled absorbance values from the experimental data, one can observe the extent by which a particular UV-Vis spectrum deviates from the model shown in **eq.1**. The observed deviations may indicate the presence of non-MN components with their own absorbance features. Figure 1 provides a general overview of the application of this

mathematical process onto an experimental UV-Vis spectrum of an unspecified MN-like material.

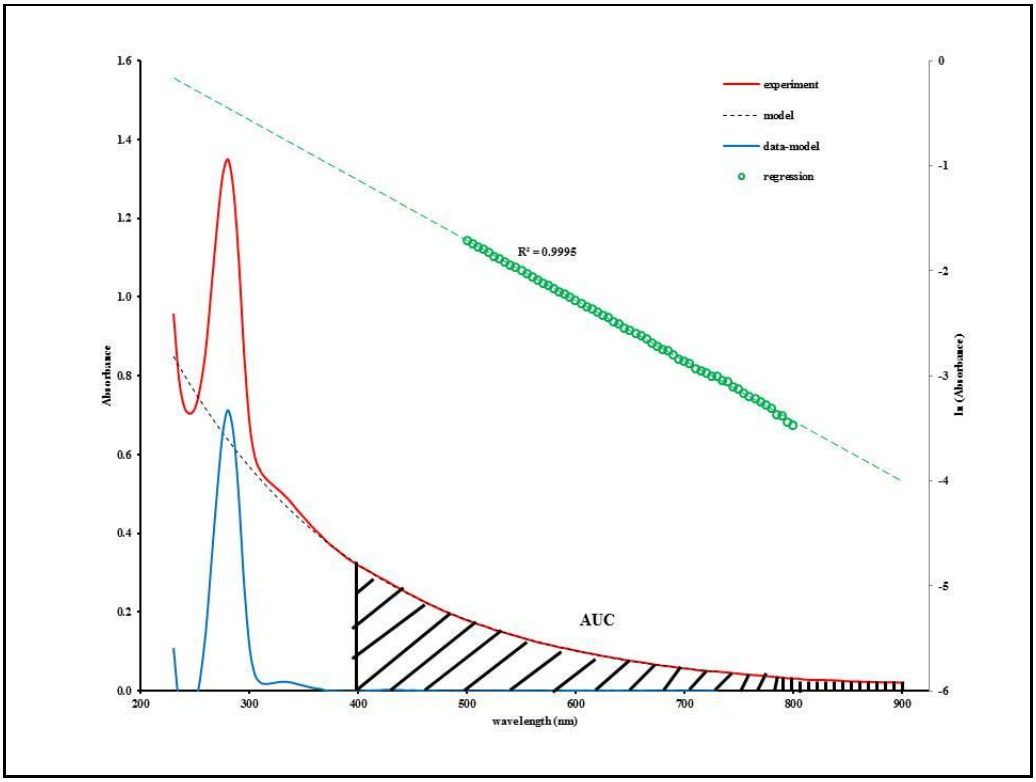

Figure 1: Red line = experimental UV-Vis spectrum of a solution containing a MN-like material. Green dots and green dotted line = linear regression process between 500nm and 800nm according to **eq.2**. Dotted black line = model of the UV-Vis spectrum based upon the constants obtained from **eq.2.** Blue line = subtraction of the modeled data (black dotted line) from the experimental data (red line). The shaded area indicates the integration according to **eq.3** between 400nm and 900nm and represents the area-under-the-curve (AUC) of the spectrum between these two wavelengths.

In this report we have applied the mathematical processing approach discussed above as a tool to compare the "darkness" of the various MN-like materials generated. In addition, we discuss our observations in the context of the UV-protective properties attributed to MN-like materials.

2. Materials and Methods

All materials, experimental conditions and collection of data were described in previous reports.[7-18] This report involves a processing of the UV-Vis spectra collected from crude reaction mixtures or from dialyzed and dried materials that were dissolved in water. Specific references and descriptions of the materials are indicated for all the results presented in this report.

3. Results

3.1 DOPA

DOPA-based MN-like materials were prepared using 0.3mM Fe^{2+} / 1.2% v/v H_2O_2, 0.3mM Fe^{2+} / 0.03% v/v H_2O_2 or 0.2M NaOH to initiate the reactions (pigments A, B or C respectively in [16]). These materials were prepared in triplicate and purified through dialysis against water. Lyophilized materials were dissolved in water to a concentration of 1 mg/mL and Figure 1 in [16] shows a photograph of these stock solutions. For all materials synthesized and purified, Vis spectra between 400 and 800nm were recorded for a dilution series with concentrations ranging from 0.02 to 1mg/mL. The mathematical process outlined in the introduction and Figure 1 was applied to all these spectra. Figure 2 presents the relationships between the average (± standard deviation; n=3) AUC calculated according to **eq.3** and the concentration of pigment for all three materials.

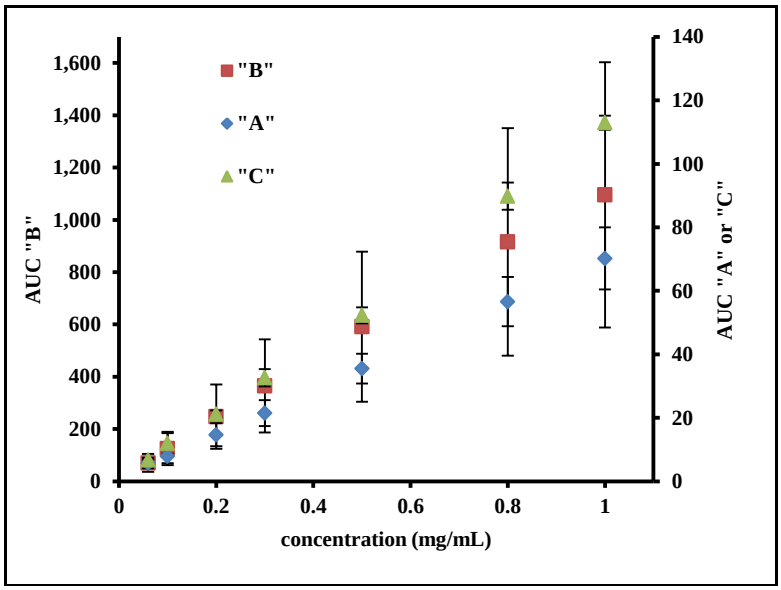

Figure 2: Average (± standard deviation; n=3) AUC calculated according to **eq.3** as a function of concentration for dialyzed and dried pigments "A", "B" and "C" from [16] dissolved in water.

The calculated values of AUC increase linearly as a function of concentration for all three pigments as is to be expected; the apparent darkness of the solutions increases with increasing concentration. The AUC values for material "B" are about 10X higher compared to the AUC values of materials "A" or "C", which is in line with the visual observations one can make from Figure 1 in [16].

In a separate set of experiments, DOPA-base, MN-like materials were synthesized using tyrosinate or a combination of Fe^{2+} and H_2O_2 as the activating agents (pigments II. III and IV in[11]). All materials were prepared in triplicate and were dialyzed against 0.3M NaCl and water as the post-reaction purification process. The lyophilized materials were dissolved in water and UV-Vis spectra were recorded between 250 and 950nm for a dilution series between 0.02 and 0.44 mg/mL. Figure 3, panels A and B, shows the processing of the spectra as outlined in the introduction and Figure 1 for pigments "II" and "IV" at 0.3 mg/mL. Figure 3, panel C, shows the relationships between the average (± standard deviation; n=3) AUC calculated according to **eq.3** and the concentration of pigment for all three materials.

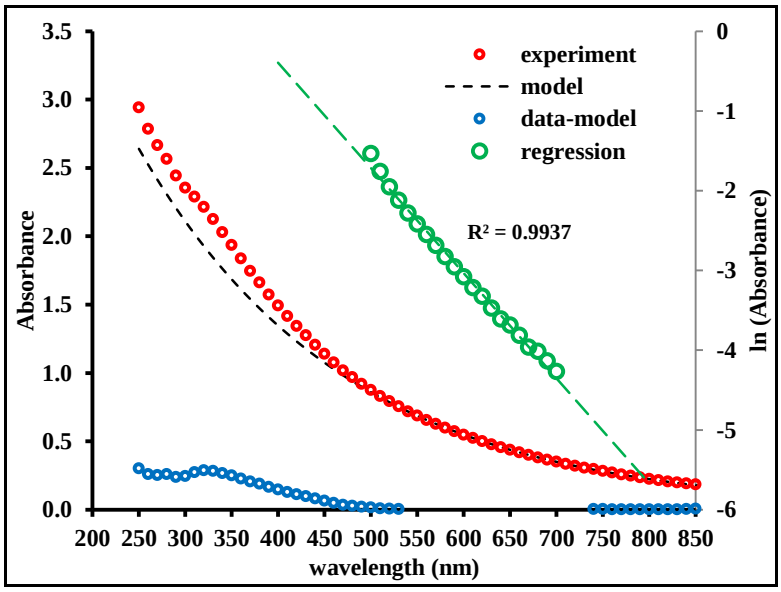

Panel A

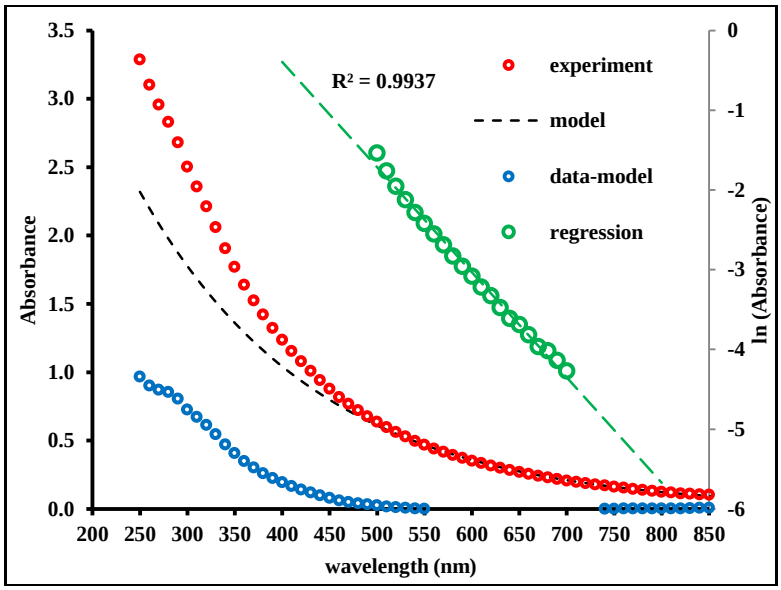

Panel B

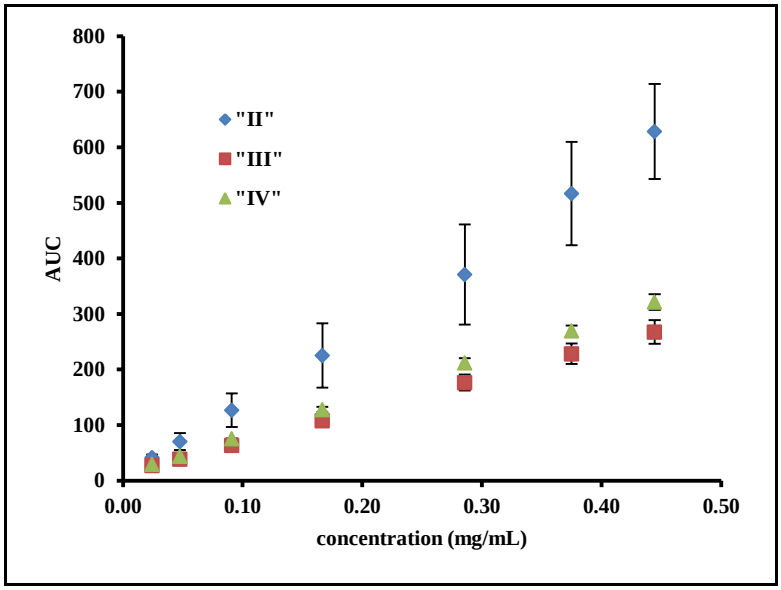

Panel C

Figure 3: Processing of UV-Vis spectra as outlined in the introduction and Figure 1 for pigment II **(panel A**) and pigment IV (**panel B**) at 0.3 mg/mL. **Panel C**: average (± standard deviation; n=3) AUC calculated according to **eq.3** as a function of concentration for pigments "II", "III" and "IV" (see [11]).

For all three types of MN-like materials prepared, the value of the calculated AUC increases with increasing concentration of the material in a linear and reproducible manner. The values of the AUC of material "II" were higher than the values of AUC obtained for materials "III" and "IV"; in line with the observed darker colors of solutions containing material "II". For pigment II (panel A in Figure 2) the approximation using **eq.1** matches the experimental data closely over

the entire UV and Vis range of the electromagnetic spectrum. This suggests that the purification process involving dialysis against salt efficiently removed non-MN components from the crude reaction mixtures. In the case of pigment IV (panel B in Figure 2) the approximation using **eq.1** deviates from the experimental data in the UV and low Vis range. This may be an indication that the purified materials still contain some non-MN components impurities following the dialysis procedures. Given the well-known cation-chelating capabilities of MNs[19-20], it is likely that the purified pigments III and IV still contain some remaining Fe cations that may be responsible for the enhanced absorption in the UV and low Vis range.

3.2 DOPA and L-cysteine

The effect of the presence of L-cysteine on the melanogenesis reaction from DOPA and other catecholamines has been studied extensively before.[7] Reaction mixtures were set up containing 2, 4, 7 or 11mM DOPA and between 0 and 16mM L-cysteine. Reactions were initiated through the presence of Na_2CO_3 and kept at 37ºC for multiple days. Vis spectra of the crude reaction mixtures were recorded between 350 and 850nm. Figure 4 illustrates the values of AUC obtained according to **eq.3** for all these crude reaction mixtures.

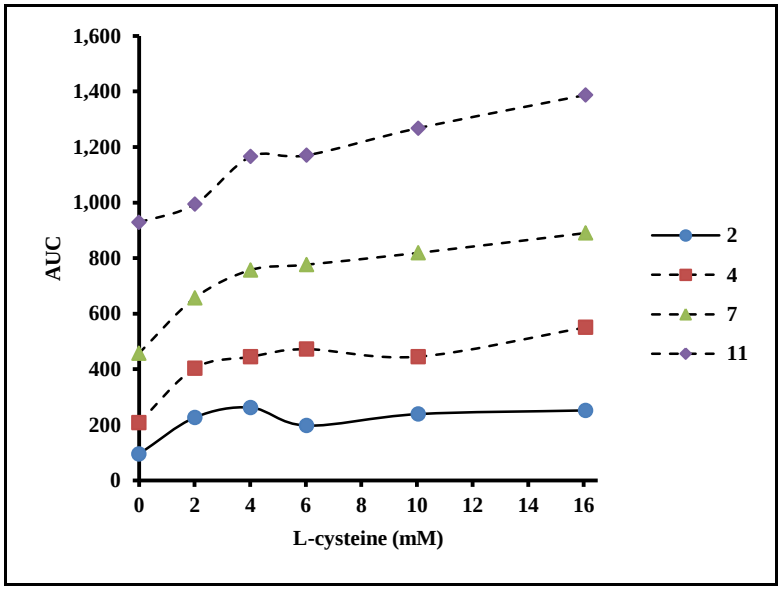

Figure 4: Values of AUC calculated according to **eq.3** for crude reaction mixtures containing 2, 4, 7 or 11mM DOPA and various concentrations of L-cysteine as discussed in [7].

The values of AUC consistently were much higher in the presence of L-cysteine compared to the reaction mixtures without any L-cysteine. However, the values of AUC did not increase

linearly with increasing concentration of L-cysteine, but appeared to reach plateau values with increasing concentrations of the amino acid. However, for any given concentration of L-cysteine, the value of AUC increased linearly with increasing concentration of DOPA (R^2 values >0.99; results not shown). The pattern of results shown in Figure 4 indicates an increased "darkness" of the reaction mixtures as a function of L-cysteine concentration which is in agreement with the visual appearance of these reaction mixtures as shown in Figure 3, panel A, of [7].

In addition to the studies discussed above, small scale, kinetic studies involving reaction mixtures containing 0.24mM DOPA and varying concentrations of L-cysteine were set up at 37ºC.[15] After three hours of reaction, UV-Vis spectra of these crude reaction mixtures were recorded. Figure 5, panels A and B, shows the processing of the spectra as outlined in the introduction and Figure 1 for the crude reaction mixtures containing 0 or 0.9mM L-cysteine.

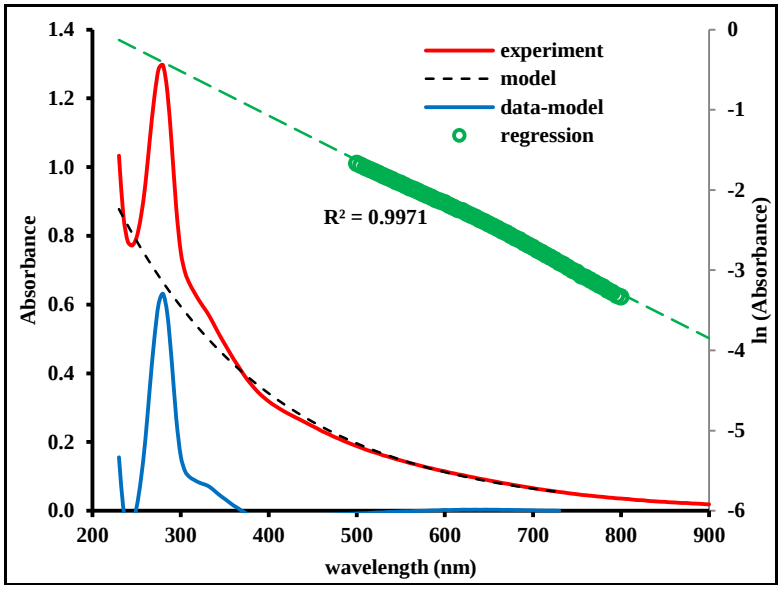

Panel A

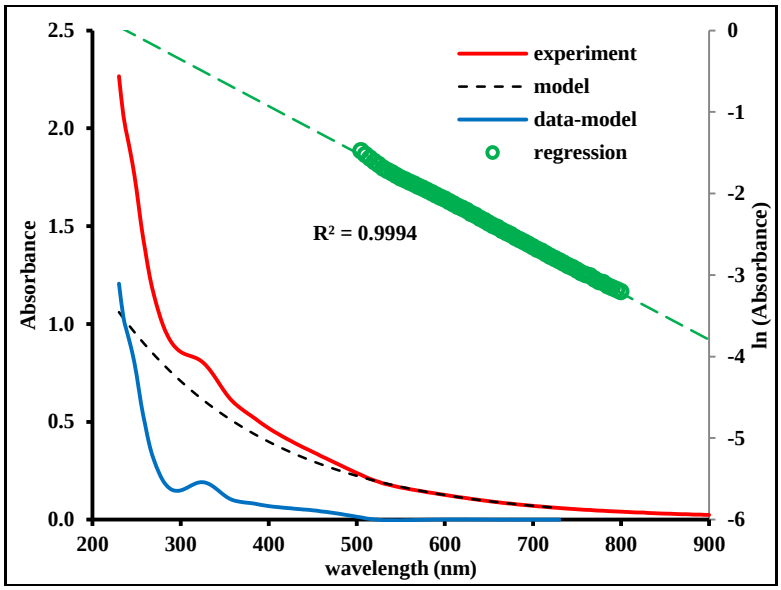

Panel B

Figure 5: Processing of UV-Vis spectra as outlined in the introduction and Figure 1 for crude reaction mixtures containing 0.24mM DOPA and 0 (panel A) or 0.9mM (panel B) L-cysteine after three hours of reaction at 37ºC; see [15].

As judged from the subtraction of the modeled data from the experimental data, the results shown in Figure 5, panel A, suggest that the melanogenesis reaction from DOPA yields components with an absorbance band around 280nm and an absorbance shoulder around 325nm. Similarly, the results presented in Figure 5, panel B, suggest that in the presence of L-cysteine, the absorbance band around 280nm is much weaker or not observed. Instead, an absorbance band around 325nm and a broad absorbance shoulder around 425nm could be observed.

3.3 Dopamine and L-cysteine

Reaction mixtures were set up containing 2, 4, 7 or 11mM dopamine and between 0 and 16mM L-cysteine.[7] Reactions were initiated by the presence of Na_2CO_3 and kept at 37ºC for multiple days. Vis spectra between 350 and 850nm were recorded of the crude reaction mixtures. Figure 6 illustrates the results of the calculations of the AUC according to **eq.3** and as outlined in the introduction.

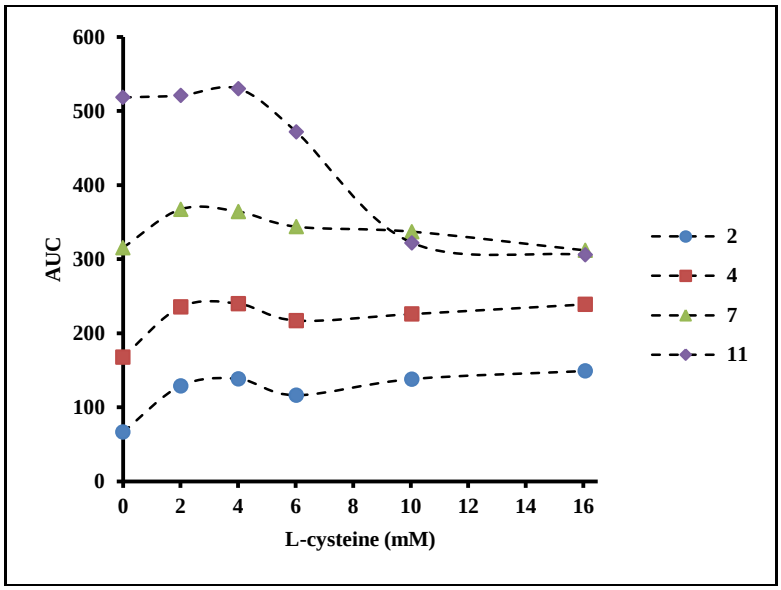

Figure 6: Values of AUC calculated according to **eq.3** for crude reaction mixtures containing 2, 4, 7 or 11mM dopamine and various concentrations of L-cysteine as discussed in [7].

At the lower concentrations of dopamine tested (2 or 4mM), the values of AUC increased with increasing concentrations of L-cysteine. This is in line with the observed increased darkness of these mixtures as shown in Figure 3, panel B of [7]. At the higher concentrations of dopamine (7 or 11mM) the values of AUC appeared to decline at the higher concentrations of L-cysteine. This is a reflection of the fact that precipitations were to be observed in the mixtures containing the higher concentrations of dopamine and L-cysteine.

In addition to the studies discussed above, small scale, kinetic studies involving reaction mixtures containing 0.24mM dopamine and varying concentrations of L-cysteine were set up at 37ºC.[15] After three hours of reaction, UV-Vis spectra of these crude reaction mixtures were recorded. Figure 7, panels A and B, shows the processing of the spectra as outlined in the introduction and Figure 1 for the crude reaction mixtures containing 0 or 0.9mM L-cysteine.

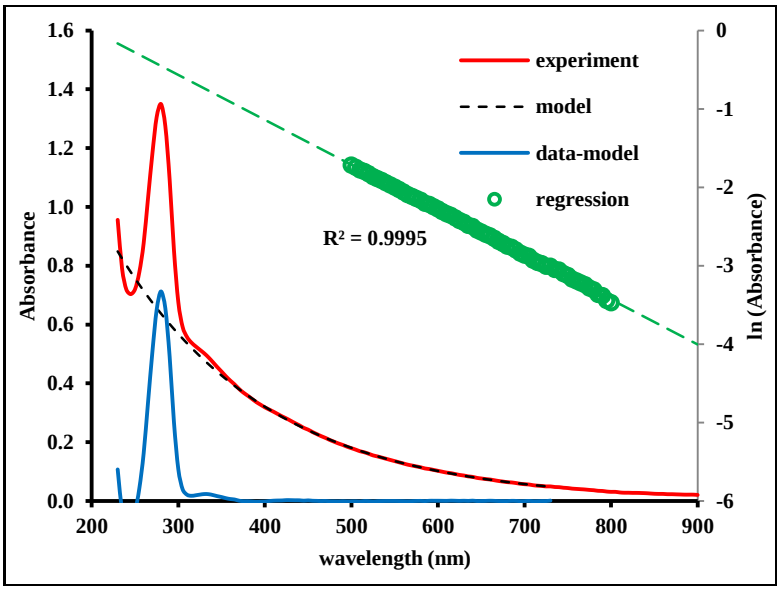

Panel A

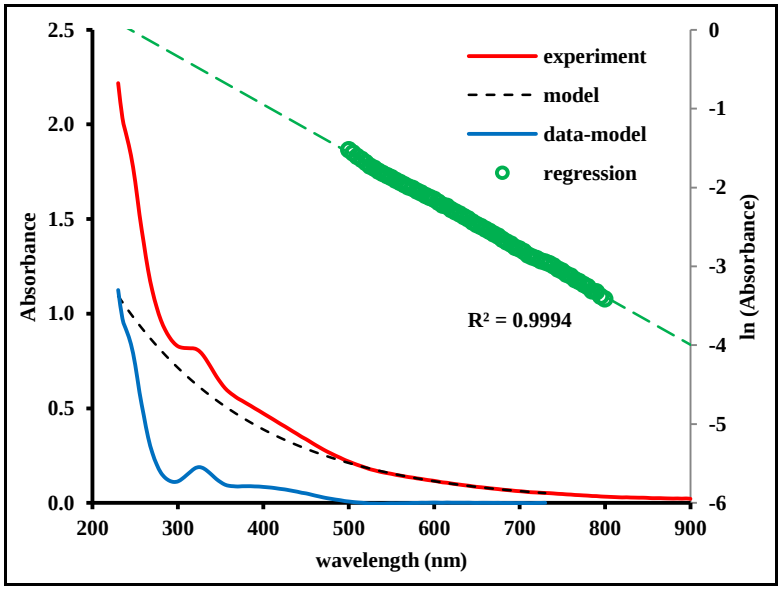

Panel B

Figure 7: Processing of UV-Vis spectra as outlined in the introduction and Figure 1 for crude reaction mixtures containing 0.24mM dopamine and 0 (panel A) or 0.9mM (panel B) L-cysteine after three hours of reaction at 37ºC; see [15].

As judged from the subtraction of the modeled data from the experimental data, the results shown in Figure 7, panel A, suggest that the melanogenesis reaction from dopamine yields components with a strong absorbance band around 280nm and a weak absorbance band around 325nm. Similarly, the results presented in Figure 6, panel B, suggest that in the presence of L-

cysteine, the absorbance band around 280nm is much weaker or not observed. Instead, an absorbance band around 325nm and a broad absorbance shoulder around 425nm can be observed. A pattern of results that is very similar to the one observed for DOPA.

3.4 Dopamine and serine, glutamine or methionine

Similar to our small-scale studies involving the effects of L-cysteine, we studied the effects of other amino acids on the kinetics of the auto-oxidation of dopamine. Reaction mixtures containing 0.24mM dopamine and varying concentrations of serine, glutamine or methionine were set up at 37ºC.[15] After three hours of reaction, UV-Vis spectra of these crude reaction mixtures were recorded. Figure 8, panels A through C, shows the processing of the spectra as outlined in the introduction and Figure 1 for the crude reaction mixtures containing 0.24mM dopamine and 31mM serine (panel A), 34mM glutamine (panel B) or 34mM methionine (panel C).

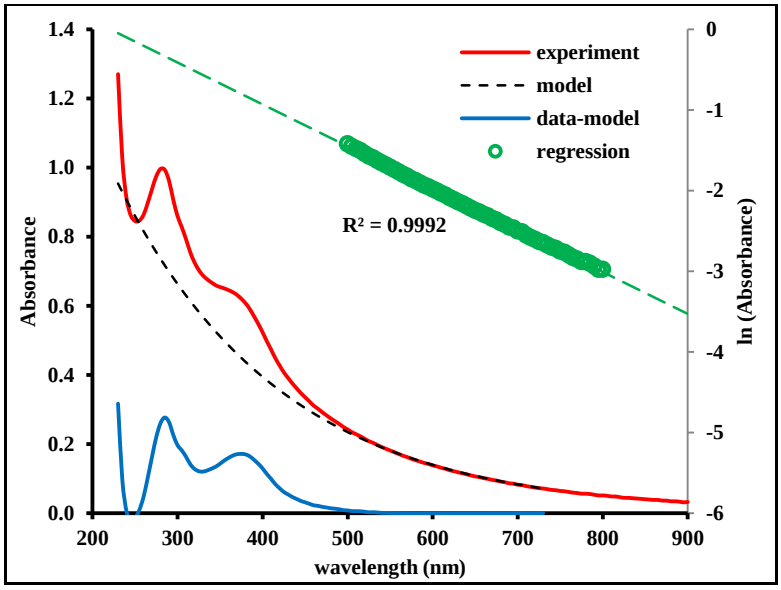

Panel A

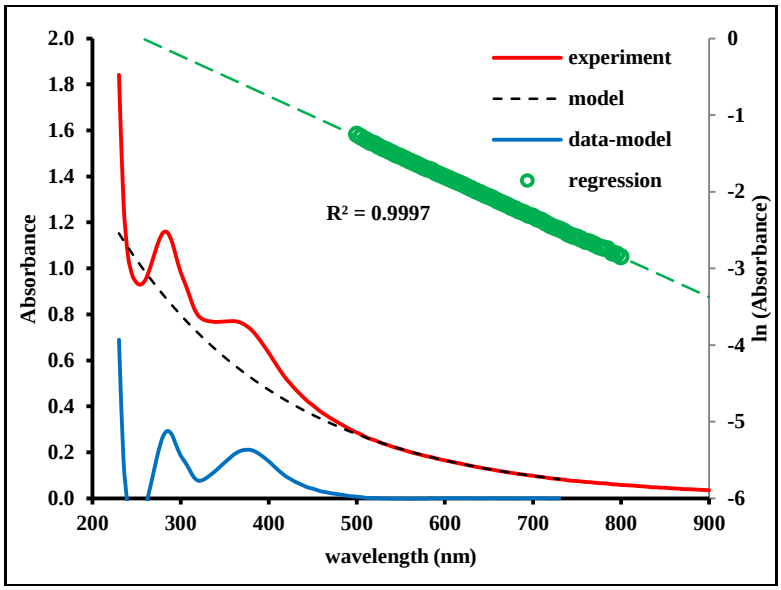

Panel B

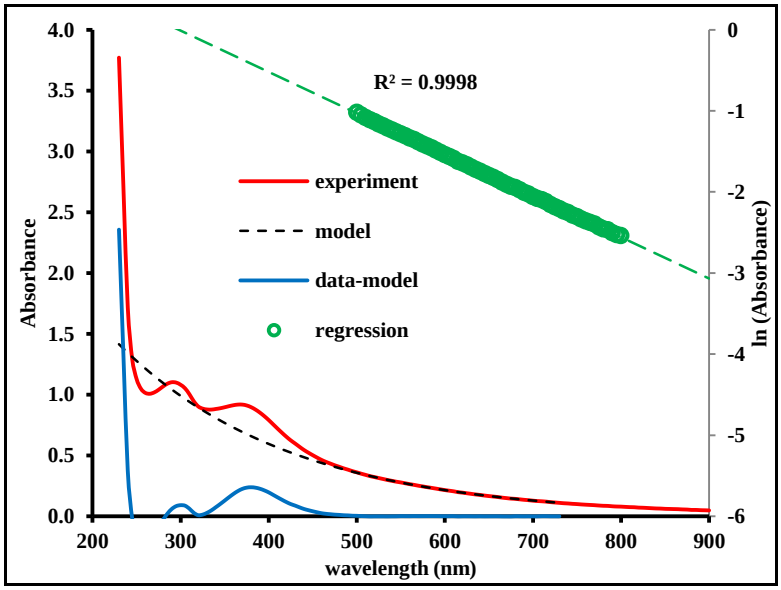

Panel C

Figure 8: Processing of UV-Vis spectra as outlined in the introduction and Figure 1 for crude reaction mixtures containing 0.24mM dopamine and 31mM serine (panel A), 34mM glutamine (panel B) or 34mM methionine (panel C) L-cysteine after three hours of reaction at 37ºC; see [15].

As judged from the subtraction of the modeled data from the experimental data, the results shown in Figure 8, panels A and B, suggest that the melanogenesis reaction from dopamine in the presence of serine or glutamine yields components with an absorbance band around 280nm and around 380nm. The case of methionine, presented in Figure 8, panel C, is different; with a

small absorbance band around 300nm and an absorbance band around 380nm. Figure 9 presents the values of the AUC calculated according to **eq. 3** for all the reaction mixtures containing 0.24mM dopamine and varying concentrations of serine, glutamine or methionine.

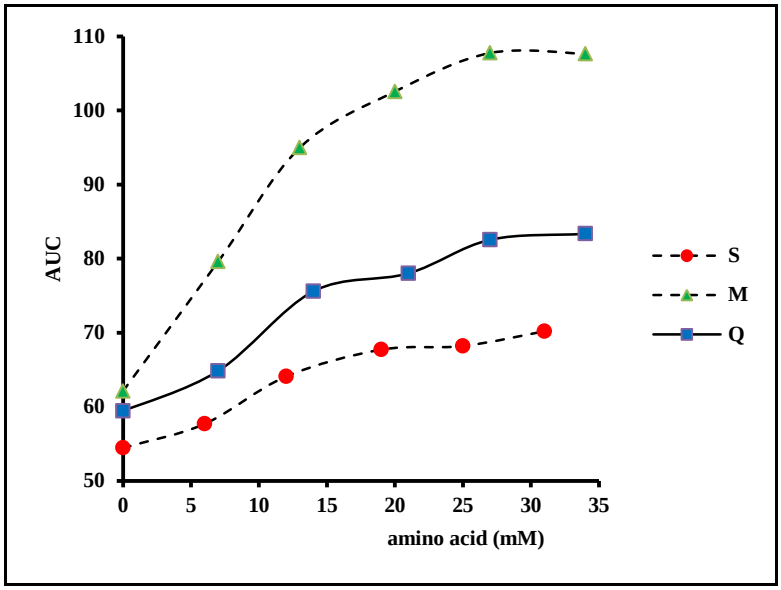

Figure 9: Values of AUC for crude reaction mixtures containing 0.24mM dopamine and varying concentrations of serine (S), glutamine (Q) or methionine (M) (see [15]).

As discussed in the introduction, the calculated values of AUC can serve as a measure of "darkness" of samples containing MN-like materials. The results presented in Figure 9 indicate that in the presence of amino acids, particularly methionine, the colors of reaction mixtures involving the auto-oxidation of dopamine appear much darker. However, it is important to point out the large excess of amino acid present in relationship to dopamine; unlike the cases of L-cysteine discussed in Figures 6 and 7.

3.5 Norepinephrine or epinephrine and L-cysteine

As for DOPA and dopamine discussed before, reaction mixtures were set up containing 2, 4, 7 or 11mM norepinephrine or epinephrine and between 0 and 16mM L-cysteine.[7] Reactions were initiated by the presence of Na_2CO_3 and kept at 37ºC for multiple days. Vis spectra between 350 and 850nm were recorded of these crude reaction mixtures. However, many of these UV-Vis spectra could not be modeled using **eq.**1 as the absorbance readings in the Vis region were barely above baseline. Only in the presence of the higher concentrations of norepinephrine or epinephrine and in the presence of L-cysteine, could reliable linear regressions according to **eq.**2

be performed. Thus, Figure 10, panels A and B, illustrates the results of the calculations of the AUC according to **eq.3** and as outlined in the introduction, but only for those reaction mixtures for which the R^2-value from the linear regression according to **eq.2** was above 0.99.

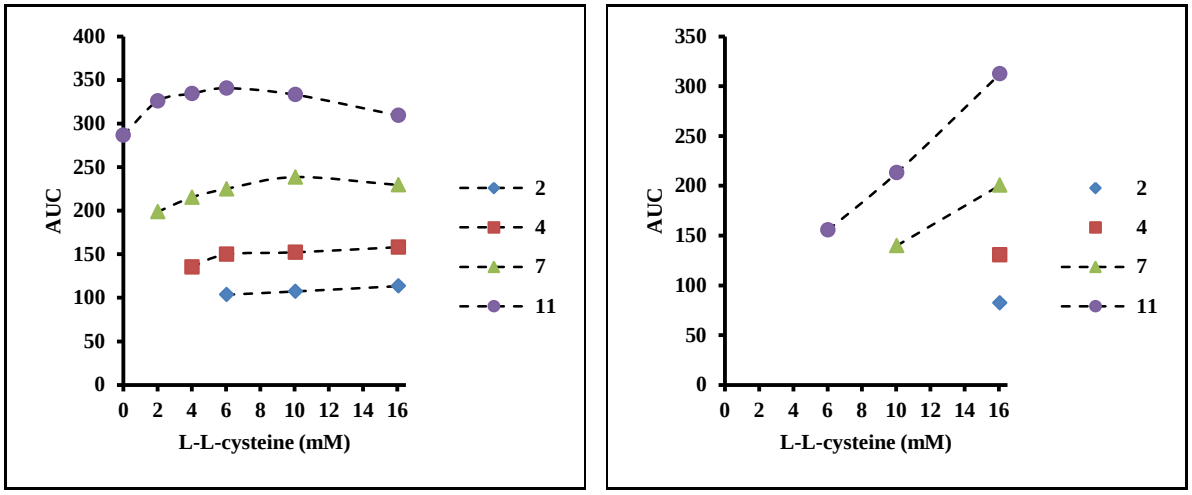

Panel A **Panel B**

Figure 10: Values of AUC for crude reaction mixtures containing 2, 4, 7 or 11mM norepinephrine (panel A) or epinephrine (panel B) and various concentrations of L-cysteine as discussed in [7].

In general, the pattern of results associated with the AUC values shown in Figure 10 is in agreement with the visual appearances of these reaction mixtures as shown in Figure 4, panels C and D, of [7].

Reaction mixtures containing 0.24mM norepinephrine or epinephrine and L-cysteine were set up and kept at 37ºC.[15] After three hours of reaction UV-Vis spectra of the crude mixtures were recorded. Figure 11, panels A through D, shows the processing of the spectra as outlined in the introduction and Figure 1 for some of these crude reaction mixtures.

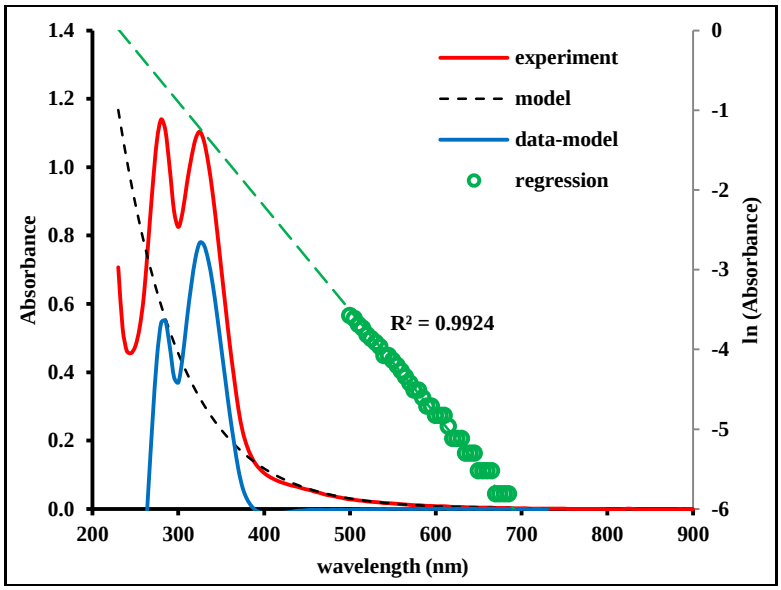

Panel A

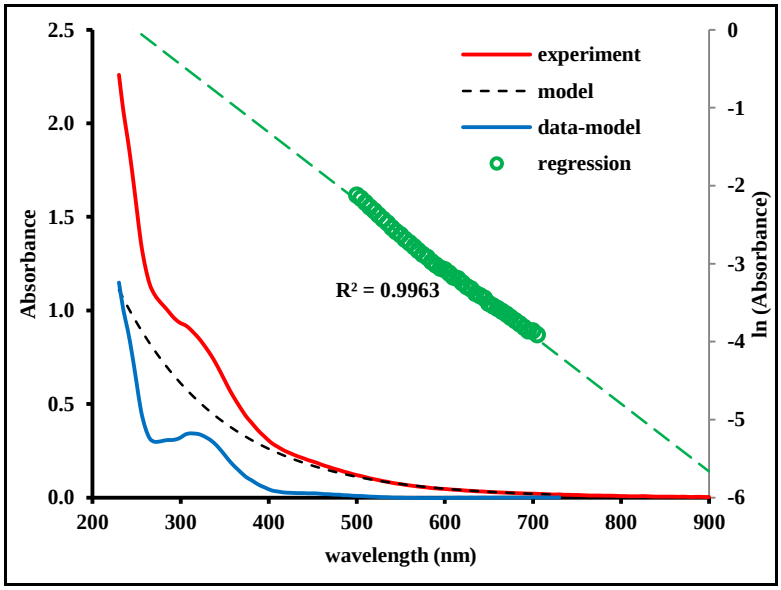

Panel B

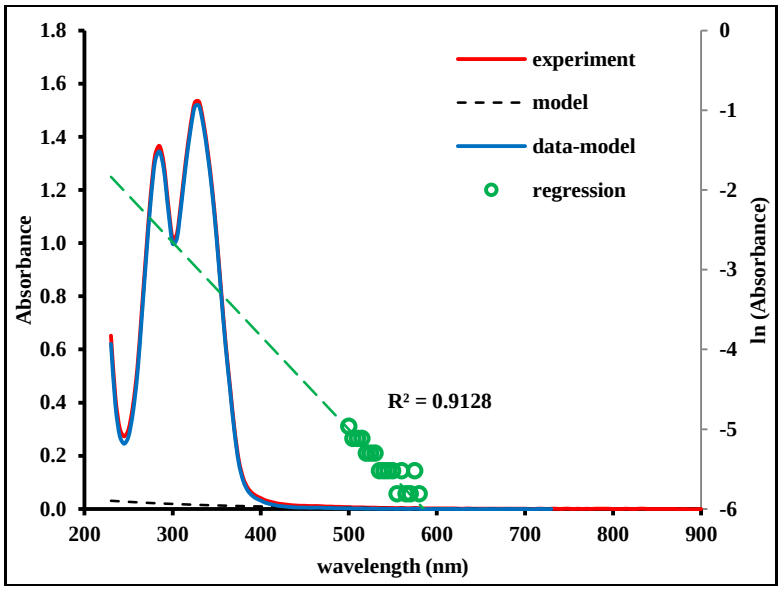

Panel C

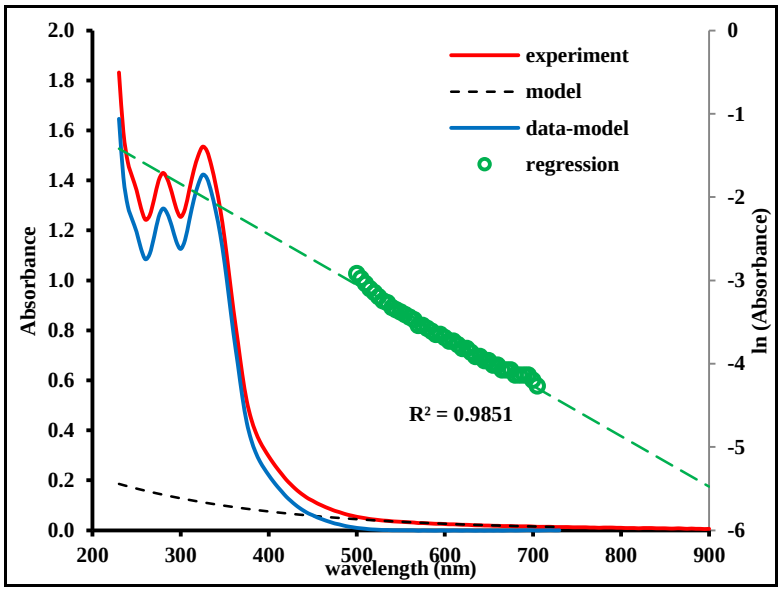

Panel D

Figure 11: Processing of UV-Vis spectra as outlined in the introduction and Figure 1 for crude reaction mixtures containing 0.24mM norepinephrine (**panel A**), 0.24mM norepinephrine and 0.6mM L-cysteine (**panel B**), 0.24mM epinephrine (**panel C**) and 0.24mM epinephrine and 0.6mM L-cysteine (**panel D**); (see [15]).

As discussed for the results presented in Figure 10, the reactions involving norepinephrine or epinephrine resulted in mixtures with much lighter colors leading to UV-Vis spectra that can not be modeled using **eq.1** with the same level of confidence as for the cases of DOPA and dopamine. In the absence of any L-cysteine, the auto-oxidation of norepinephrine and

epinephrine results in components with strong absorbance bands around 280 and 325nm. The presence of L-cysteine appeared to impact this pattern in the case of norepinephrine, but much less in the case of epinephrine.

3.6 Miscellaneous experiments

In a variety of experiments, other catecholic compounds were subjected to oxidation reactions leading to MN-like materials that were purified through dialysis against water and characterized.[13-14] These characterizations involved, in part, dissolving the purified and dried materials into water and recording their UV-Vis spectra. Figure 12, panels A through G, illustrate some of the results thus obtained for solutions containing 0.2 mg/mL of these MN-like materials.

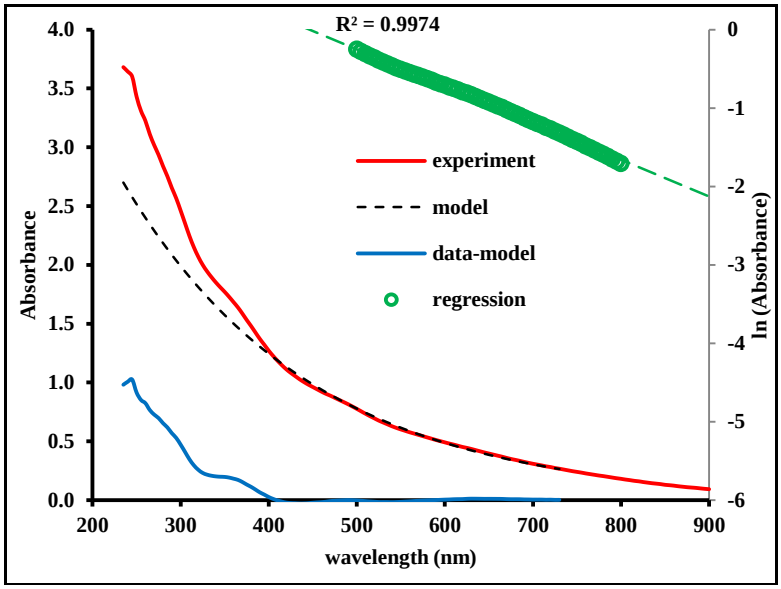

Panel A

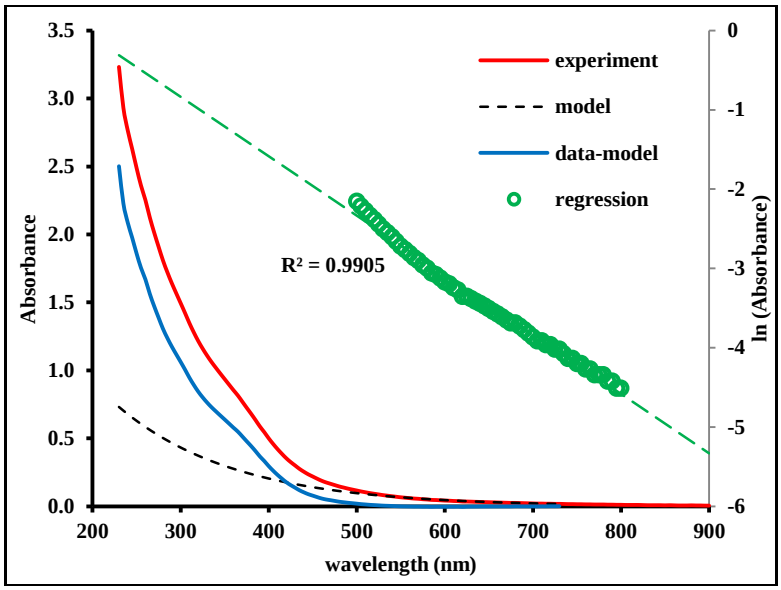

Panel B

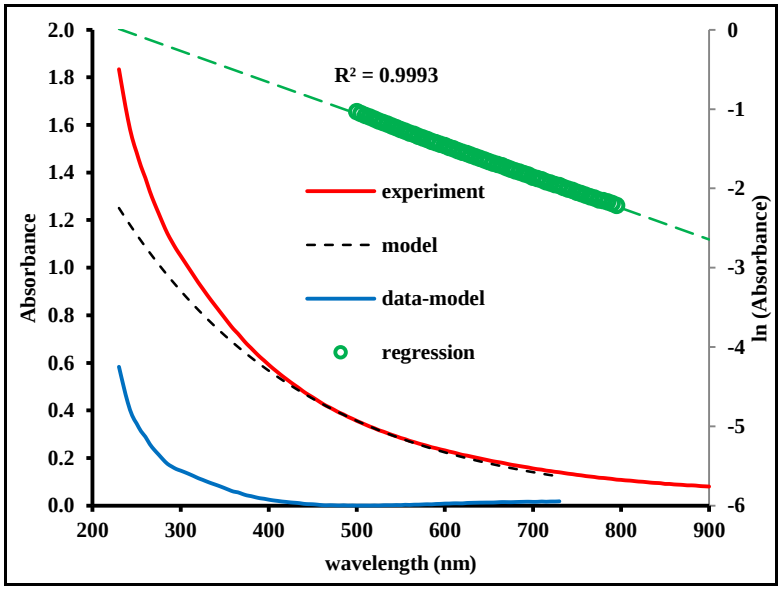

Panel C

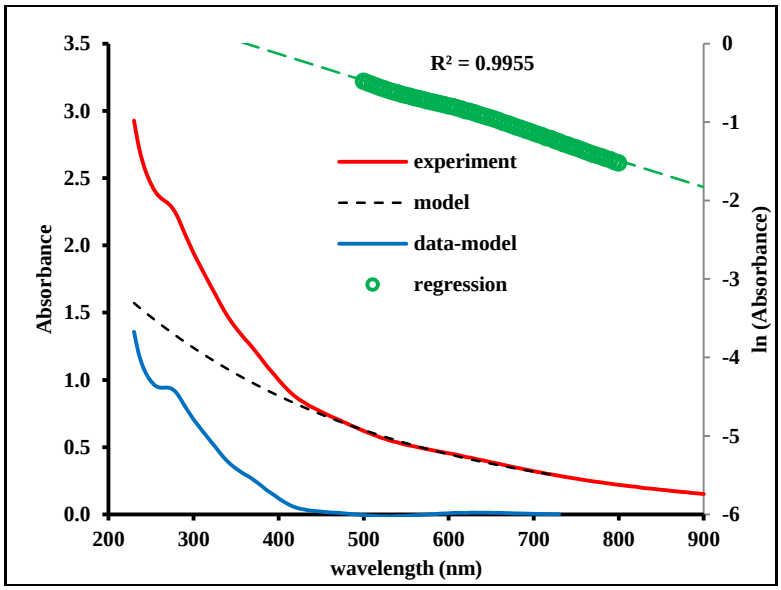

Panel D

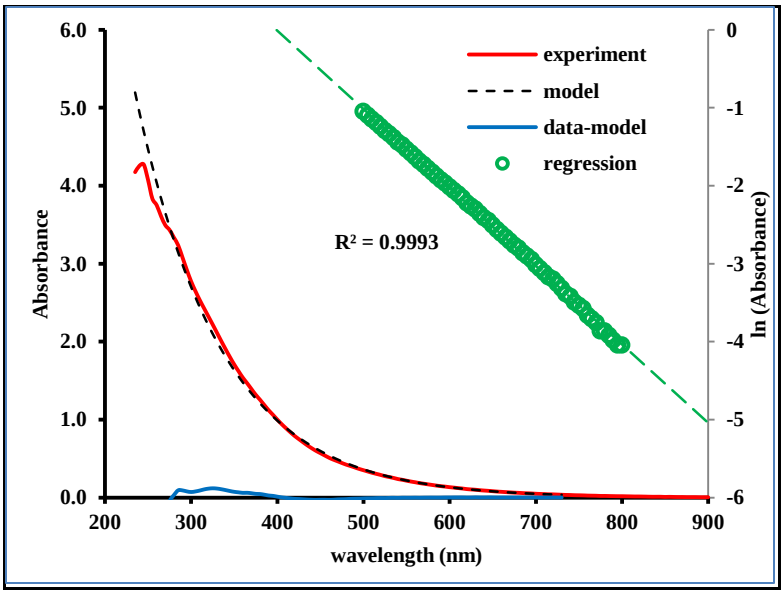

Panel E

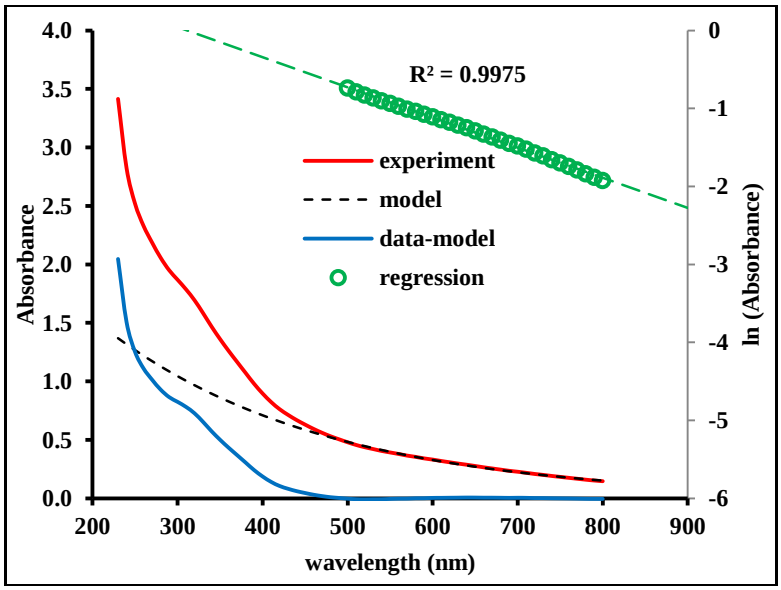

Panel F

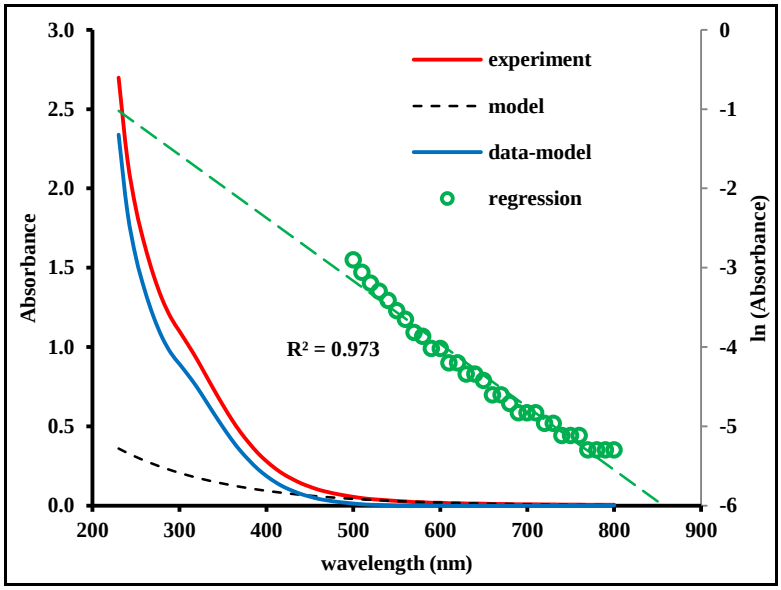

Panel G

Figure 12: Processing of UV-Vis spectra as outlined in the introduction and Figure 1 for: **Panel A:** MN-like material made from homogentisic acid in the presence of 0.3mM Fe^{2+} and 0.1% v/v H_2O_2 dissolved in water at 0.2 mg/mL(see [14]). **Panel B:** MN-like material made from homogentisic acid in the presence of 0.3mM Fe^{2+} and 1.2% v/v H_2O_2 dissolved in water at 0.2 mg/mL(see [14]). **Panel C:** MN-like material made from 5-hydroxy indole in the presence of 0.3mM Fe^{2+} and 1.2% v/v H_2O_2 dissolved in water at 0.2 mg/mL. **Panel D:** MN-like material made from catechol in the presence of 0.3mM Fe^{2+} and 0.06% v/v H_2O_2 dissolved in water at 0.2 mg/mL (see [13]). **Panel E:** MN-like material made from catechol in the presence of 0.3mM Fe^{2+} and 1.2% v/v H_2O_2 dissolved in water at 0.2 mg/mL (see [13]). **Panel F:** MN-like material made from pyrogallol in the presence of 0.3mM Fe^{2+} and 0.06% v/v H_2O_2 dissolved in water at 0.2 mg/mL (see [13]). **Panel G:** MN-like material made from pyrogallol in the presence of 0.3mM Fe^{2+} and 1.2% v/v H_2O_2 dissolved in water at 0.2 mg/mL (see [13]).

Depending on the precursor used or the oxidation reaction conditions employed, the experimental data fit the model of **eq.1** more or less better. Particularly good fits were obtained for both 5-hydroxy indole (panel C) and catechol (panel E) when using relatively high levels of H_2O_2 (1.2% v/v) as the oxidizing agent.

In the cases of pyrogallol and catechol, a broader range of MN-like materials were synthesized, purified and characterized. These materials were synthesized using varying concentrations of H_2O_2 as the oxidizing agent.[13] The UV-Vis spectra of the materials, dialyzed against water, dried and dissolved in water at a concentration of 0.2mg/mL were recorded. These spectra were processed to calculate their AUC values as outlined in the introduction and using **eq.3**. Figure 13 illustrates, for both compounds, the relationship between the AUC values and the concentration of H_2O_2 used to synthesize the materials.

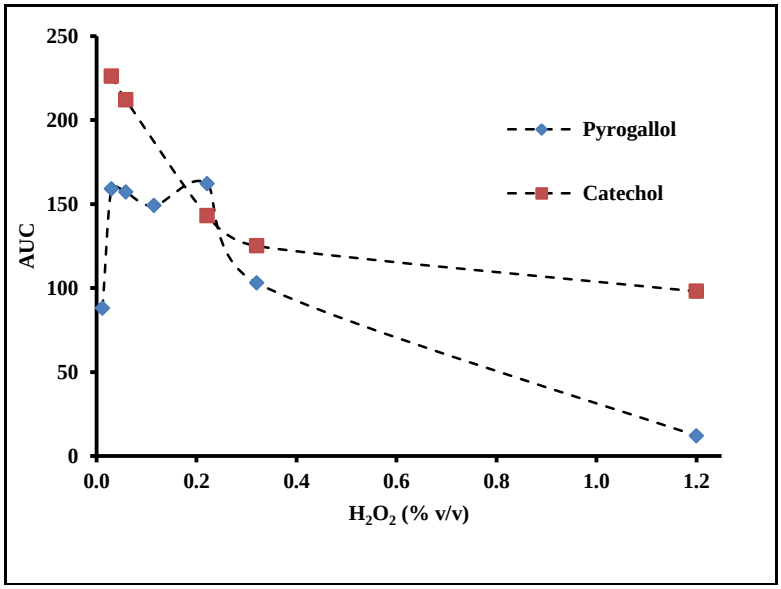

Figure 13: Relationship between % H_2O_2 used in the synthesize of MN-like materials from pyrogallol or catechol and the AUC values calculated according to **eq.3** from UV-Vis spectra of the materials dissolved in water at 0.2mg/mL.

In general, depending on the concentration of H_2O_2 employed, darker or lighter materials can be synthesized from both precursors. For the most part, it appears that lighter-colored materials are obtained when using pyrogallol than when using catechol as the precursor.

In conclusion, Figure 14 presents a comparison of the AUC values of the various purified MN-like materials, dissolved in water at 0.2 mg/mL, discussed in this report.

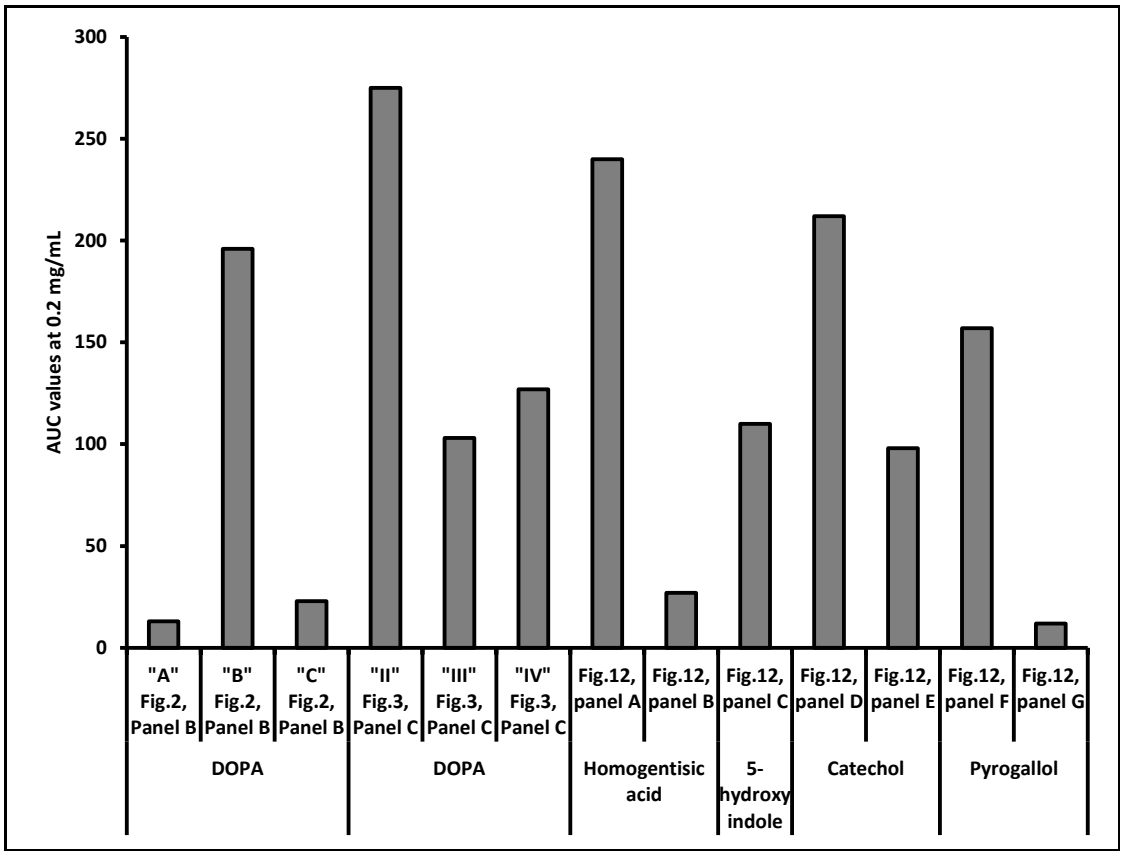

Figure 14: Comparison of the AUC values of MN-like materials dissolved in water at 0.2mg/mL synthesized from various precursors or under varying reaction conditions as discussed throughout this report. For the DOPA-based samples, extrapolations were performed based upon the linear relationships shown in Figures 2 and 3 to estimate their AUC values at 0.2 mg/mL.

The results shown in Figure 14 are illustrative of the wide range of "darkness" MN-like materials can possess depending on the precursor used and the reaction conditions employed to generate the MN.

4. Discussion

The many important functions and potential applications attributed to MNs have been discussed extensively elsewhere.[20-26] However, new insights obtained in our laboratory suggest that the melanogenesis reaction involving the auto-oxidation of catecholamines into MN-like materials leads to a hybrid substance consisting of two classes of components: a) darkly colored, insoluble components (iMN) and b) nearly colorless, soluble components (sMN). [7] The sMN appear to contain unoxidized precursor units and may well function to stabilize, i.e. keep in suspension, the iMN. The iMN can be separated from the sMN through a co-precipitation

process involving insoluble inorganic salts like $CaCO_3$.[7] The sMN components exhibit strong absorbance bands in the UV region of the electromagnetic spectrum, but appear not to contribute much to the overall color or "darkness" of the MN-like material generated during the melanogenesis reaction. All the dark color resides in the iMN fraction, but this fraction may not be the major product generated. Thus, when evaluating any function or application of MN materials, one does have to consider the importance or non-importance of the different fractions, sMN vs. iMN, that may be present in the MN-like material synthesized. Or in other words: When does the dark color of any MN material matter vis-à-vis their function or application?

MNs play a very important function as a main pigment to provide coloration for camouflage, visual signaling or other purposes.[27] Changes in coloration can be controlled through chemical or physical means. One possible chemical control mechanism may be the synthesis of MN-like materials with varying intensity of darkness through the use of different precursors, oxidation mechanisms or reaction conditions, e.g., presence of amino acids, as outlined in this and associated reports. In this regard, the color of the material generated is of importance. All too often, melanogenesis is studied using DOPA or dopamine as the precursor. However, in nature other precursors could be used to generate MNs, e.g., in the cases of bacterial or fungal MN. In addition, *in vivo* melanogenesis reactions occur in the midst of a complex biochemical environment. The effect of other biomolecules, e.g., amino acids, proteins, polysaccharides, on the melanogenesis reaction and the physic-chemical properties of the final product is neglected.

MNs exhibit a broad-band absorbance profile over the entire UV-Vis range of the electromagnetic spectrum. This property makes MN materials suitable for absorbing radiation energy and dispersing it[28] or using it as part of an organism's thermoregulation needs.[29-30] In a similar context, the presence of MN may provide an organism with enhanced protection against ionizing radiation.[31-32] For all these types of applications, the "darkness" of the MN material may be of crucial importance. More commonly, MNs are often described as natural sunscreens, capable of absorbing and dissipating UV radiation and providing protection against the damaging effects of the UV light on the integrity of DNA.[33-35] According to the World Health Organization (WHO) website*, solar UV radiation is divided into three fractions: 1) UVC (100-280nm) which does not reach the Earth's surface as it is blocked by the chemicals of the atmosphere, 2) UVB

* https://www.who.int/uv/uv_and_health/en/#:~:text=The%20UV%20region%20covers%20the,(100%2D280%20nm).

(280-315nm) which does reach the Earth's surface to some degree and 3) UVA (315-400nm). DNA molecules absorb strongly in the UVC region, but as this type of UV light does not reach the Earth's surface, it is of little concern. DNA does absorb UVB to some degree and UVA minimally.[36-37] However, given that the sun's UVA radiation does reach the Earth's surface to a significant extent, it is of importance to consider the effect of this type of UV radiation on the chemical integrity of DNA inside cells.[36] Figure 5, panel A, and Figure 7, panel A, show typical UV-Vis spectra of crude reaction mixtures obtained from the auto-oxidation of DOPA or dopamine respectively. Both exhibit a similar profile: a combination of a monotonic, broad-band absorption feature and a strong absorbance band around 280nm. This first feature we attribute to the presence of iMN, while the latter we attribute to the presence of sMN containing unoxidized precursor units. From this perspective it appears that the sMN portion possesses a strong UV-absorbing capacity and as such may provide a strong protective capacity; particularly against the UVB portion of the UV radiation. However, the absorption of the UVB energy may lead to an increase in temperature of the cell/organism and without the dissipation of this thermal energy damage to a cell/organism may still occur. In this context, the presence of the iMN portion may assist in the dissipation of the thermal energy that may arise from the UV absorption by the sMN. For both DOPA and dopamine, the melanogenesis reaction in the presence of L-cysteine results in a material with a much darker appearance. However, the strong absorbance band around 280nm is absent or much smaller, while the absorbance capacity around 325nm and the 400nm region appears to be more prominent (see Figure 5, panel B and Figure 7, panel B). Thus, such materials could provide less protection against UVB radiation, but more protection against UVA radiation. In the case of melanogenesis from dopamine in the presence of amino acids other than L-cysteine, the absorbance band around 280nm decreased, but an increased absorbance in the 350 to 425nm region is to be observed (see Figure 8). Similarly as for the effect of L-cysteine, MNs created in the presence of amino acids, albeit at much higher concentrations compared to L-cysteine, could lead to materials that provide increased protection against UVA radiation, but less against UVB radiation.

In the cases of norepinephrine or epinephrine the melanogenesis reaction appears to lead to less iMN and more sMN components with strong absorbance bands around 280nm and 350nm; covering much of the UVB and UVA spectrum (see Figure 11, panels A and C). The presence of L-cysteine has a dramatic effect on the UV absorbance profile in the case of norepinephrine (see

Figure 11, panel B), but much less so in the case of epinephrine (see Figure 11, panel D). At first glance it would appear that the components generated from epinephrine through the melanogenesis reaction are more suitable to provide protection against a wide range of UV radiation. However, without or with less presence of iMN components to dissipate the thermal energy resulting from the absorption of the UV radiation, damage because of increase temperatures could still occur. Melanogenesis reactions starting from epinephrine in the presence of L-cysteine do result in enhanced formation of iMN, as exhibited in the darker colors of these reaction mixtures.

The points regarding the UV protection provided by MN-like materials we raised in this discussion are to be classified as hypotheses. However, it adds to a recommendation made in an earlier report that when studying the melanogenesis reaction, *in vitro* or *in vivo*, one needs to look "behind" the colors of the MNs and consider the nature and properties of the colorless components generated.[7]

References

1.Ito, S.; Wakamatsu, K., Chemistry of mixed melanogenesis--pivotal roles of dopaquinone. *Photochem Photobiol* **2008,** *84* (3), 582-92.

2.Ito, S.; Wakamatsu, K., Chemistry of Melanins. In *The Pigmentary System*, Nordlund, J. J.; Boissy, R. E.; Hearing, V. J.; King, R. A.; Oetting, W. S.; Ortonne, J., Eds. Blackwell Publishing Ltd: 2007; pp 282-310.

3.Ju, K. Y.; Fischer, M. C.; Warren, W. S., Understanding the Role of Aggregation in the Broad Absorption Bands of Eumelanin. *ACS Nano* **2018,** *12* (12), 12050-12061.

4.Meredith, P.; Sarna, T., The physical and chemical properties of eumelanin. *Pigment Cell Research* **2006,** *19* (6), 572-594.

5.Sarna, T.; Swartz, H. A., The Physical Properties of Melanins. In *The Pigmentary System*, Nordlund, J. J.; Boissy, R. E.; Hearing, V. J.; King, R. A.; Oetting, W. S.; Ortonne, J., Eds. Blackwell Publishing Ltd: 2007; pp 311-341.

6.Meredith, P.; Powell, B. J.; Riesz, J.; Nighswander-Rempel, S. P.; Pederson, M. R.; Moore, E. G., Towards structure–property–function relationships for eumelanin. *Soft Matter* **2006,** *2* (1), 37-44.

7.Vercruysse, K.; Govan, V., Melanogenesis: A Search for Pheomelanin and Also, What Is Lurking Behind Those Dark Colors? *ChemRxiv* **2019**.

8.Vercruysse, K., Synthesis of L-DOPA based pigments with different physic-chemical properties. *ChemRxiv* **2018**.

9.Vercruysse, K., Preliminary Observations on the Interactions Between Chlorogenic Acid and Select Amino Acids. *ChemRxiv* **2019**.

10.Vercruysse, K.; Clark, A.; Alatas, N.; Brooks, D.; Hamza, N.; Whalen, M., Polysaccharide-mediated synthesis of melanins from serotonin and other 5-hydroxy indoles. *BioRxiv* **2017**.

11.Vercruysse, K.; Moore, J., Synthesis of L-DOPA Based Melanins with Reproducible Physic-Chemical Properties. *ChemRxiv* **2018**.

12.Vercruysse, K.; Richardson, N., Melanogenesis Using Tyrosinate (Not Tyrosinase). *ChemRxiv* **2018**.

13.Vercruysse, K.; Russell, S.; Knight, J.; Stewart, N.; Wilson, N.; Richardson, N., Dark- or Light-Colored Melanins: Generating Pigments Using Fe^{2+} and H_2O_2. *ChemRxiv* **2017**.

14.Vercruysse, K.; Taylor, A.; Knight, J., Fe^{2+}/H_2O_2-mediated oxidation of homogentisic acid indicates the production of ochronotic and non-ochronotic pigments. Implications in Alkaptonuria and beyond. *BioRxiv* **2017**.

15.Vercruysse, K.; Venise, G.; Stenesha, F., Kinetic Study of the Melanogenesis from Select Catecholamines in the Presence of L-Cysteine or Other Amino Acids. *ChemRxiv* **2020**.

16.Vercruysse, K.; Whalen, M., Light- or Dark-Colored, L-DOPA-Based Melanins. *ChemRxiv* **2018**.

17.Vercruysse, K. P.; Clark, A. M.; Bello, P. A. F.; Alhumaidi, M., Using size exclusion chromatography to monitor the synthesis of melanins from catecholamines. *J Chromatogr B* **2017,** *1061-1062*, 11-16.

18.Vercruysse, K. P.; Farris, T. S.; Whalen, M. M., Interleukin-1β and -6 release from immune cells by DOPA-based melanin as free pigment or complexed to carboxymethylcellulose. *BioRxiv* **2017**.

19.Zucca, F. A.; Segura-Aguilar, J.; Ferrari, E.; Munoz, P.; Paris, I.; Sulzer, D.; Sarna, T.; Casella, L.; Zecca, L., Interactions of iron, dopamine and neuromelanin pathways in brain aging and Parkinson's disease. *Prog Neurobiol* **2017,** *155*, 96-119.
20.Solano, F., Melanins: Skin Pigments and Much More—Types, Structural Models, Biological Functions, and Formation Routes. *New Journal of Science* **2014,** *2014*, 498276.
21.Huang, L.; Liu, M.; Huang, H.; Wen, Y.; Zhang, X.; Wei, Y., Recent Advances and Progress on Melanin-like Materials and Their Biomedical Applications. *Biomacromolecules* **2018,** *19* (6), 1858-1868.
22.Ball, V., Polydopamine Nanomaterials: Recent Advances in Synthesis Methods and Applications. *Frontiers in Bioengineering and Biotechnology* **2018,** *6* (109).
23.Solano, F., Melanin and Melanin-Related Polymers as Materials with Biomedical and Biotechnological Applications-Cuttlefish Ink and Mussel Foot Proteins as Inspired Biomolecules. *Int J Mol Sci* **2017,** *18* (7).
24.d'Ischia, M., Melanin-Based Functional Materials. *Int J Mol Sci* **2018,** *19* (1).
25.Turick, C. E.; Knox, A. S.; Becnel, J. M.; Ekechukwu, A. A.; Milliken, C. E., Properties adnd Function of Pyomelanin. In *Biopolymers*, Inashar, M., Ed. InTech: 2010; pp 449-472.
26.Liu, H.; Yang, Y.; Liu, Y.; Pan, J.; Wang, J.; Man, F.; Zhang, W.; Liu, G., Melanin-Like Nanomaterials for Advanced Biomedical Applications: A Versatile Platform with Extraordinary Promise. *Advanced Science* **2020,** *7* (7), 1903129.
27.Duarte, R. C.; Flores, A. A. V.; Stevens, M., Camouflage through colour change: mechanisms, adaptive value and ecological significance. *Philos Trans R Soc Lond B Biol Sci* **2017,** *372* (1724), 20160342.
28.Pinkert, S.; Zeuss, D., Thermal Biology: Melanin-Based Energy Harvesting across the Tree of Life. *Current Biology* **2018,** *28* (16), R887-R889.
29.Cordero, R. J. B.; Robert, V.; Cardinali, G.; Arinze, E. S.; Thon, S. M.; Casadevall, A., Impact of Yeast Pigmentation on Heat Capture and Latitudinal Distribution. *Curr Biol* **2018,** *28* (16), 2657-2664 e3.
30.Delhey, K., Darker eggs feel the heat. *Nature ecology & evolution* **2020,** *4* (1), 22-23.

31.Pacelli, C.; Bryan, R. A.; Onofri, S.; Selbmann, L.; Shuryak, I.; Dadachova, E., Melanin is effective in protecting fast and slow growing fungi from various types of ionizing radiation. *Environ Microbiol* **2017,** *19* (4), 1612-1624.
32.Casadevall, A.; Cordero, R. J. B.; Bryan, R.; Nosanchuk, J.; Dadachova, E., Melanin, Radiation, and Energy Transduction in Fungi. *Microbiol Spectr* **2017,** *5* (2).
33.Brian Nofsinger, J.; Simon, J. D., Radiative Relaxation of Sepia Eumelanin is Affected by Aggregation. *Photochemistry and Photobiology* **2001,** *74* (1), 31-37.
34.d'Ischia, M.; Wakamatsu, K.; Cicoira, F.; Di Mauro, E.; Garcia-Borron, J. C.; Commo, S.; Galván, I.; Ghanem, G.; Kenzo, K.; Meredith, P.; Pezzella, A.; Santato, C.; Sarna, T.; Simon, J. D.; Zecca, L.; Zucca, F. A.; Napolitano, A.; Ito, S., Melanins and melanogenesis: from pigment cells to human health and technological applications. *Pigm Cell Melanoma Res* **2015,** *28* (5), 520-544.
35.Marchetti, B.; Karsili, T. N. V., Theoretical insights into the photo-protective mechanisms of natural biological sunscreens: building blocks of eumelanin and pheomelanin. *Phys Chem Chem Phys* **2016,** *18* (5), 3644-3658.
36.Schuch, A. P.; Moreno, N. C.; Schuch, N. J.; Menck, C. F. M.; Garcia, C. C. M., Sunlight damage to cellular DNA: Focus on oxidatively generated lesions. *Free Radical Biology and Medicine* **2017,** *107*, 110-124.
37.Rastogi, R. P.; Richa; Kumar, A.; Tyagi, M. B.; Sinha, R. P., Molecular mechanisms of ultraviolet radiation-induced DNA damage and repair. *J Nucleic Acids* **2010,** *2010*, 592980-592980.